Chapter-5

STUDIES ON SPECTRAL CHARACTERIZATION, CRYSTAL STRUCTURE NUCLEASE ACTIVITY AND CYTOTOXICITY OF DINUCLEAR COPPER(II) COMPLEXES FORMED WITH TRIDENTATE LIGANDS

Introduction:

Studies on mononuclear copper(II) complexes of tridentate NNO donor Schiff base ligands (SAMEN, SAPEN, HAPMEN and HAPPEN) were presented in previous Chapter. Nuclearity of the complexes depends upon the conditions and reagents employed in the synthesis of complexes. When $Cu(NO_3)_2.3H_2O$ was made to react with tridentate ligands [Chapter – 3, section 3 (ii)] it results in the formation of mononuclear metal complexes. The same ligands when reacted with $CuClO_4.6H_2O$ in presence of triethylamine yields in the formation of dinuclear copper(II) complexes. These complexes are characterized by physico-chemical and spectral techniques viz., IR, UV-visible and ESR spectroscopy. Structure of dinuclear copper complex with 2-[1-(propylamino-ethylimino)-methyl]-phenol (SAPEN) was determined by single crystal X--ray diffraction method. Electrochemical behavior of these complexes was investigated by cyclic voltammetric studies. Binding interactions of metal complexes with calf-thymus DNA are determined using absorption spectrophotometry. Cleavage activities of these complexes are investigated on a double stranded pBR plasmid DNA by using gel electrophoresis experiments in the absence and in the presence of an oxidant (H_2O_2), a complexing agent (EDTA), a free radical scavenger (DMSO) and a reducing agent (DTT). Syntheses of ligands and complexes are given in Chapter – 3.

As reported in Chapter-3 (Section 3 ii), the ligands SAMEN, SAPEN, HAPMEN and HAPPEN were obtained as viscous liquids. General structure of the ligands can be shown as:

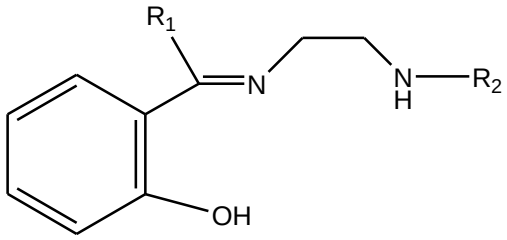

General structure of ligands

Ligand	**R_1**	**R_2**
SAMEN	H	CH_3
SAPEN	H	C_3H_7
HAPMEN	CH_3	CH_3
HAPPEN	CH_3	C_3H_7

a. Physico-chemical properties

Synthesis of metal complexes was given in Chapter-3 (Section 3 ii). All the complexes are stable at room temperature, non-hygroscopic, soluble in water, methanol, DMF and DMSO. Analytical and physico-chemical properties of complexes are given in **Table 5.1**.

b. Conductivity measurements

Conductivity measurements of the complexes were performed by dissolving the complexes in DMF. Molar conductance values of Cu(II) complexes suggest that these complexes are electrolytes. The data are incorporated in **Table 5.1**.

c. Magnetic susceptibility measurements

Magnetic susceptibility values of all the complexes were determined at 300K in solid state. The magnetic moment values of copper complexes are found to be sub-normal to spin only value [1-4]. The values are found to be in the range of 1.16 to 1.24 BM. The data reveal that these complexes are dimeric and there is a strong metal-metal interaction between the two copper centers. The magnetic susceptibility data are shown in **Table 5.1**.

Table 5.1

Analytical and Physico-chemical properties of copper (II) complexes

Complex	Mol. Formula	Colour (Yield%)	Decomposition Temp. °C	Magnetic Moment μ_{eff} (BM)	Molar conductivity ($\Omega^{-1}cm^2mol^{-1}$)	Elemental analysis			
						C%	H%	N%	Cu%
$[Cu(SAMEN)]_2 2ClO_4$	$C_{20}H_{26}Cl_2Cu_2N_4O_{10}$	Green (52)	255-257	1.22	86.3	35.27 (35.41)	3.94 (3.82)	7.97 (8.23)	18.75 (18.67)
$[Cu(SAPEN)]_2 2ClO_4$	$C_{24}H_{34}Cl_2Cu_2N_4O_{10}$	Green (69)	242-244	1.14	81.8	39.26 (39.14)	4.58 (4.65)	7.66 (7.61)	17.16 (17.26)
$[Cu(HAPMEN)]_2 2ClO_4$	$C_{22}H_{30}Cl_2Cu_2N_4O_{10}$	Dark green (66)	270-272	1.23	85.6	37.46 (37.28)	4.27 (4.23)	7.75 (7.91)	17.89 (17.95)
$[Cu(HAPPEN)]_2 2ClO_4$	$C_{26}H_{38}Cl_2Cu_2N_4O_{10}$	Dark green (68)	285-287	1.26	79.5	40.89 (40.83)	4.87 (4.97)	7.45 (7.34)	16.65 (16.63)

d. Electronic spectra

Electronic absorption spectra of copper(II) complexes were recorded in H_2O and DMF. The important electronic spectral data of copper(II) complexes are presented in **Table 5.2.** The electronic spectrum of $[Cu(HAPPEN)]_2\ 2ClO_4$ complex is shown in **Fig 5.1**. In aqueous solution all the complexes show strong intense bands in the region 36549-37548 cm^{-1} (λ = 266 – 273 nm) attributed due to intraligand and π-π^* aromatic ring and imine moiety, one medium intensity band observed in the region 27548-28818 cm^{-1} (λ = 347 – 363 nm) is due to metal to ligand charge transfer transition (MLCT). Whereas one broad band observed in the region 16447-16722 cm^{-1} (λ = 598-608 nm) is assigned to d-d transition. In DMF the absorption bands are shifted to higher wavelengths suggesting the involvement of solvent molecules in coordination. Bathochromic shift of absorption bands in d-d transition region is $\Delta\lambda$ = 6 – 13 nm. The electronic spectra copper(II) complexes display weak d - d band in the low intensity in 16233-16393 cm^{-1} region assigned to $^2E_g \rightarrow {}^2T_{2g}$ electronic transition in favour of octahedral structure in DMF medium. Six coordination for copper(II) is facilitated by axial coordination of DMF solvent molecules.

Table 5.2: Electronic spectral data (cm^{-1}) of copper (II) complexes

Complex	$\pi - \pi^*$		Charge transfer (MLCT)		d – d	
	H_2O	DMF	H_2O	DMF	H_2O	DMF
$[Cu(SAMEN)]_2\ 2ClO_4$	37174 (269)	36900 (271)	27624 (362)	27397 (365)	16447 (608)	16233 (616)
$[Cu(SAPEN)]_2\ 2ClO_4$	36549 (273)	36496 (274)	27548 (363)	27174 (368)	16639 (601)	16286 (614)
$[Cu(HAPMEN)]_2\ 2ClO_4$	37336 (267)	37174 (269)	27933 (358)	27397 (365)	16500 (606)	16366 (611)
$[Cu(HAPPEN)]_2\ 2ClO_4$	37548 (266)	37313 (268)	28818 (347)	27322 (366)	16722 (598)	16393 (610)

Wavelengths (λ) in nm are shown in parantheses

Approximate ε (lit. $mol^{-1}.cm^{-1}$) values are: ~2000, ~ 680, ~ 35 for $\pi - \pi^*$~, MLCT and d – d transitions respectively.

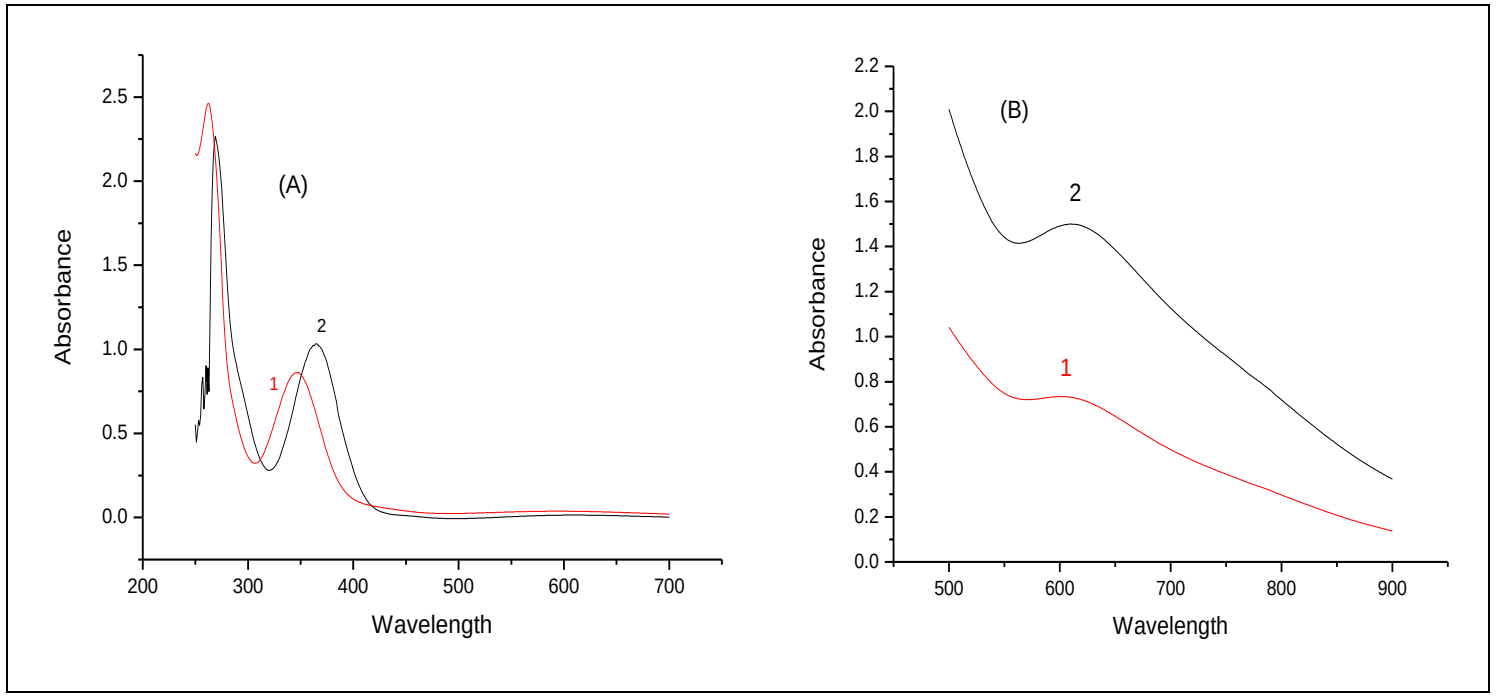

Fig 5.1: (A) Electronic spectrum of $[Cu(HAPPEN)]_2\ 2ClO_4$ in H_2O (1) in DMF (2)

(B) Spectrum of highly concentrated solution

e. Infrared spectra

Important IR spectral bands and their tentative assignments are given in **Table 5.3.** Typical FT-IR spectrum of $[Cu(SAMEN)]_2\ 2ClO_4$ is shown in **Fig 5.2**. Infrared spectra of all the complexes show a broad band observed in the region 3413 – 3436 cm^{-1} may be assigned to ν(NH) vibration of the ligands. Sharp absorption bands in the range 1584 – 1637 cm^{-1} are assigned to coordinated azomethine ν(C=N) group. When ClO_4^- ions are considered, ν_3 mode bands in the region 1077 – 1115 cm^{-1} are slightly broadened, but the ν_4 bands in the region 624 – 626 cm^{-1} is the devoid of any splitting and is consistent with the IR normal modes for a T_d symmetry, suggesting that these anions $[ClO_4^-]$ are not coordinated to the metal atom [5].

Table 5.3: Important IR spectral bands and their tentative assignments

Complex	$\nu_{(NH)}$	$\nu_{(C=N)}$	$\nu_{(ClO4)}$	$\nu_{(M-O)}$	$\nu_{(M-N)}$
$[Cu(SAMEN)]_2\ 2ClO_4$	3436	1637	1087 & 624	505	467
$[Cu(SAPEN)]_2\ 2ClO_4$	3413	1626	1115 & 625	499	458
$[Cu(HAPMEN)]_2\ 2ClO_4$	3434	1596	1088 & 626	501	455
$[Cu(HAPPEN)]_2\ 2ClO_4$	3415	1584	1077 & 626	502	458

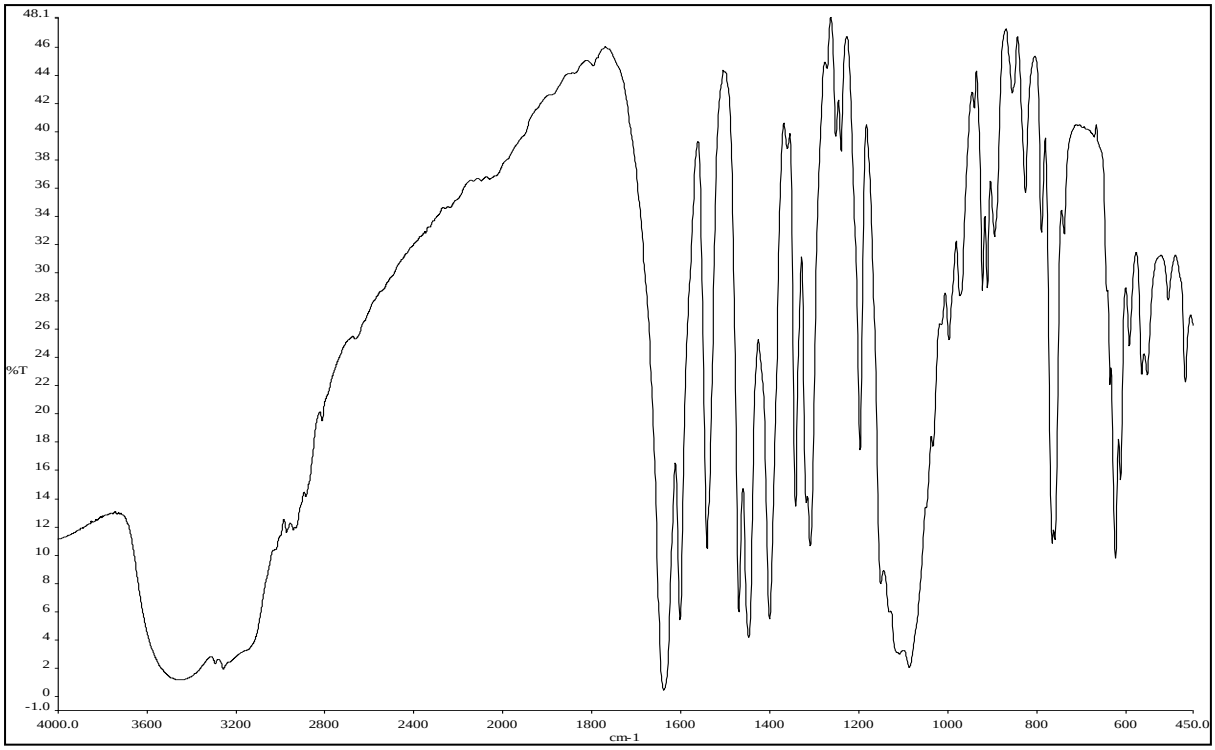

Fig 5.2: Typical FT-IR spectrum of $[Cu(SAMEN)]_2\ 2ClO_4$

f. ESR spectral studies

The ESR spectra of copper complexes were recorded in Varian E-112 X-band spectrophotometer at room temperature and liquid nitrogen temperature (LNT) in both solution ((DMF) and solid state.

Typical X-band ESR spectra of $[Cu(HAPPEN)]_2\ 2ClO_4$ complex is shown in **Fig 5.3**. The spin Hamiltonian and orbital reduction parameters of mononuclear complexes are given in **Table 5.4**. The $g_{\parallel}$ and $g_{\perp}$ values are computed from the spectra using (TCNE) free radical as 'g' marker. It is significant from the Table 5.4 that the observed values for all these complexes are less than 2.3 suggesting covalent character of the metal-ligand bonding. The g tensor values of copper(II) complexes can be used to derive the ground state. From the observed values of complexes at 300K and 77K in solid state spectrum it is clear that $g_{\parallel} > g_{\perp} > 2.00$ which suggests the fact that the unpaired electrons lies predominantly in the

$d_{x^2-y^2}$ orbital [6]. For ESR spectra at 77 K and 300 K, the 'G' values are found to be less than 4, which suggests that there is considerable interaction between copper(II) ions in the solid state which further supports the dinuclear nature of the complexes. In the solid state, similar spectra of these complexes at 77K and 300K indicates the geometry around copper(II) ion is unaffected on cooling to liquid nitrogen temperature.

The solution EPR spectra recorded in DMF, shows four-hyperfine signals which were not observed in DMF at 77 K. The spin-orbit coupling constant, λ value of the complexes calculated using the relations, $g_{av} = 1/3[g_{\parallel} + 2g_{\perp}]$ and $g_{av} = 2(1-2\lambda/10Dq)$, is less than the free Cu(II) ion (-832cm^{-1}) which also supports the covalent nature of M-L bond in the complexes [7]. The observed $K_{\parallel} < K_{\perp}$ relation in all the complexes indicates the presence of in-plane π-bonding [7]. Also, the observed $g_{\parallel}$ values of less than 2.3 provide evidence for the covalent character of bonding between Cu(II) ion and the ligand [8]. Increasing steric hindrance caused by bulky ligands results in the lowest $A_{\parallel}$ and highest $g_{\parallel}$ values. The in-plane bonding parameter α^2 values are calculated using the following relation:

$$\alpha^2 = - (A_{\parallel}/0.036) + (g_{\parallel} - 2.0023) + 3/7\ (g_{\perp} - 2.0023) + 0.04.$$

Table 5.4:

Spin Hamiltanian and orbital reduction parameters for copper (II) complexes at 300 and 77 K in solid state and in DMF solution

Complex	In solid state				In DMF solution										
	$g_{\parallel}$	$g_{\perp}$	g_{av}	G	$g_{\parallel}$	$g_{\perp}$	g(av)	G	λ	$K_{\parallel}$	$K_{\perp}$	$A_{\parallel}$ cm^{-1}	$A_{\perp}$ cm^{-1}	A_{av}	α^2
$[Cu(SAMEN)]_2 2ClO_4$	2.066	2.049	2.055	1.344	2.204	2.098	2.133	2.107	541	0.871	1.429	0.0134	0.0062	0.0086	0.523
$[Cu(SAPEN)]_2 2ClO_4$	2.079	2.056	2.064	1.428	2.127	2.059	2.081	2.199	331	0.874	1.179	0.0072	0.0051	0.0058	0.391
$[Cu(HAPMEN)]_2 2ClO_4$	2.070	2.057	2.062	1.247	2.198	2.082	2.120	2.496	494	0.901	1.147	0.0131	0.0060	0.0084	0.635
$[Cu(HAPPEN)]_2 2ClO_4$	2.080	2.054	2.061	1.506	2.126	2.054	2.078	2.392	319	0.890	1.151	0.0065	0.0031	0.0043	0.366

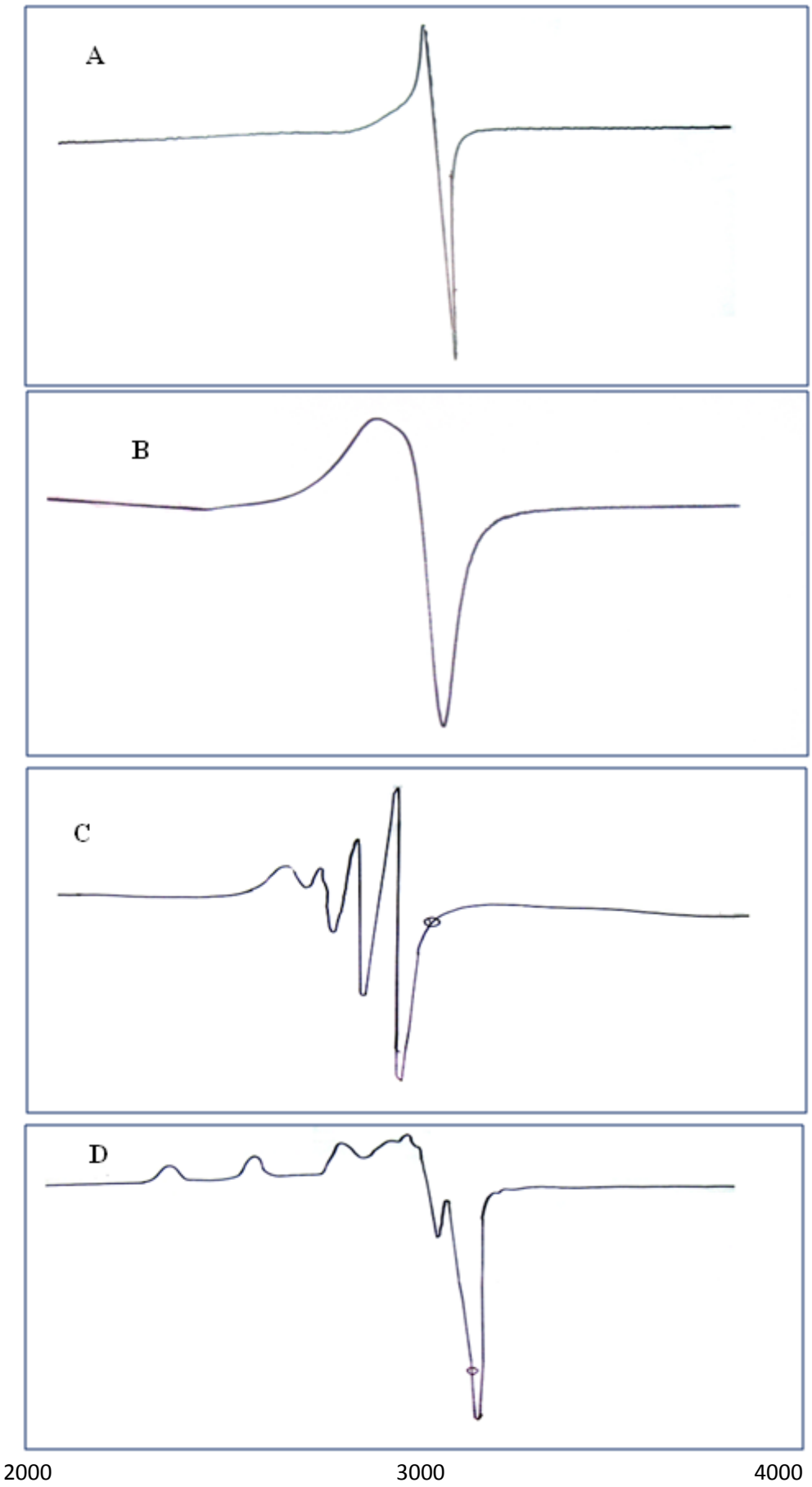

Fig 5.3: (A) X-band powder ESR spectra of $[Cu(HAPPEN)]_2$ $2ClO_4$ at 300K, (B) at LNT, (C) in DMF solution at 300K and (D) at LNT in DMF solution

Based on molar conductance, magnetic susceptibility measurements, IR and ESR data, it is suggested that all the copper(II) complexes have dimeric square-planar structure containing oxo bridges as suggested below:

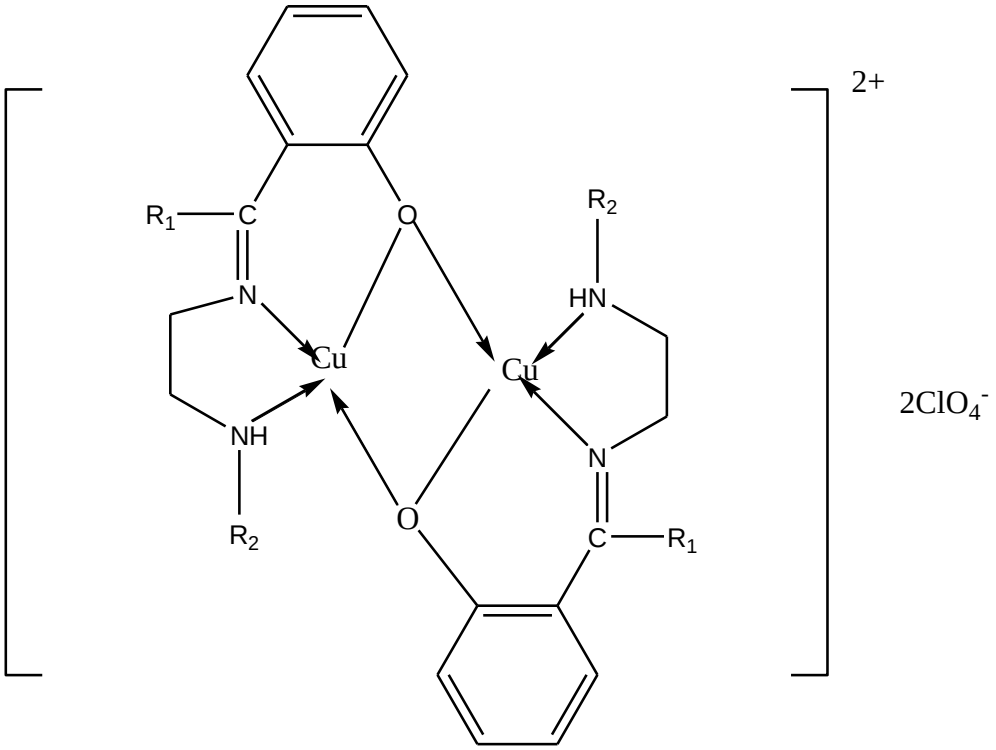

Where R_1 = H/CH_3 and R_2 = CH_3/ C_3H_7

Fig 5.4: Tentative structure of dinuclear copper(II) complex

g. Single crystal X-ray studies

Isolation of single crystals

In spite of repeated efforts to isolate the single crystals of all the complexes, only copper(II) complex of the ligand SAPEN could be isolated as single crystal suitable for X-ray diffraction studies. Deep green hexagonal single crystals of the complex were grown in acetonitrile solution on slow diffusion with n-hexane.

Description of crystal structure of $[Cu(SAPEN)]_2\ 2ClO_4$

The complex crystallizes in monoclinic, space group P21/c with the unit cell parameters; a = 11.9790(5) Å, b = 14.7940(5) Å, c = 17.0060(6) Å, $\alpha = \gamma = 90°$ and β=102.040(10), V=2946.46(19) $Å^3$, Z=4. Crystal data and structure refinements are shown in **Table. 5.5**. The structure is shown in **Fig 5.5** together with the numbering scheme in the metal coordination sphere. Close packing diagram of the complex is shown in **Fig 5.6.**

Dinuclear cation of the complex comprises two [Cu(SAPEN)] subunits, which are interconnected through two oxygen bridges afforded by the oxygen atoms of the ligands. The copper center has square-planar geometry with the coordination to two nitrogen atoms and one oxygen atom from the tridentate ligand while the oxygen atoms of the ligands forming bridges in between the two Cu atoms. In the cation $[(CuSAPEN)]_2^{2+}$ the average bond lengths in the square planar coordination sphere are Cu–N(amino) 2.0045 Å, Cu–N(imino) 1.927 Å, Cu–O(ligand) 1.9367 Å, and Cu–O(axial) 1.9537 Å respectively. The axial Cu–O bonds are longer than those of equatorial oxygen atoms of the ligands. The bond distance between the two copper atoms is 2.9278 Å. Selected bond lengths and selected bond angles are presented in **Tables 5.6** and **5.7** respectively.

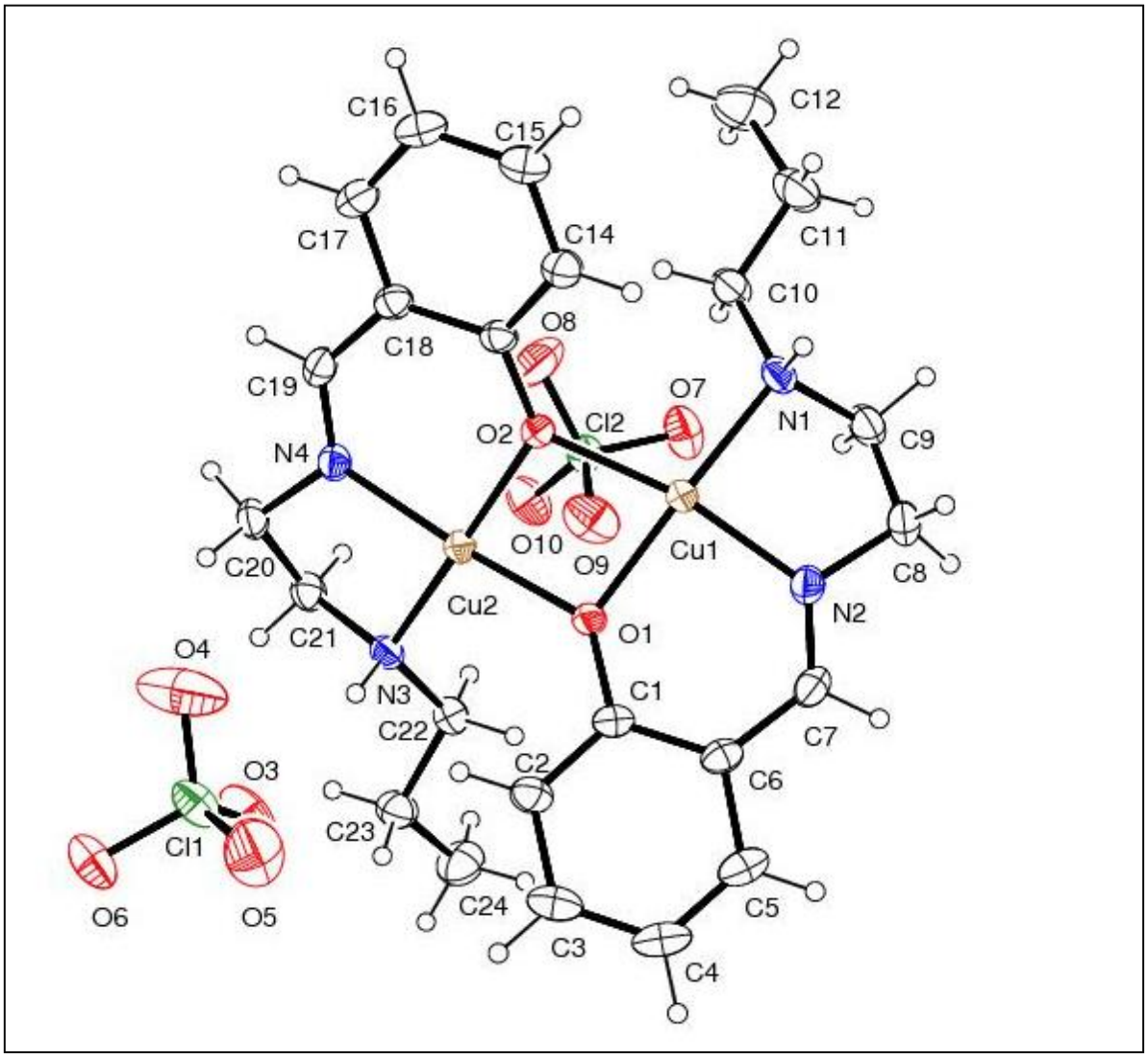

Fig 5.5: ORTEP view of the $[Cu(SAPEN)]_2\ 2ClO_4$ complex

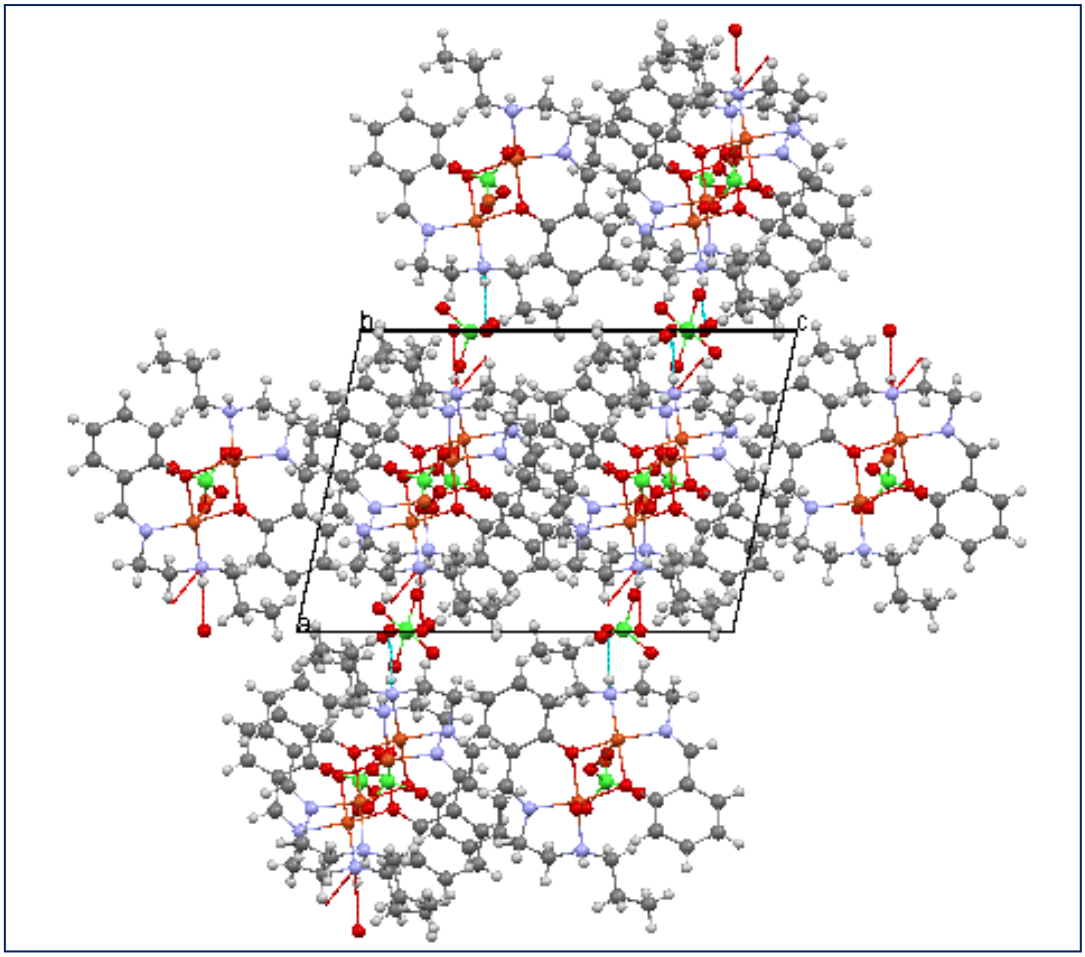

Fig 5.6: Close packing diagram of $[Cu(SAPEN)]_2$ $2ClO_4$

Table 5.5: Crystal data and structure refinement for $[Cu(SAPEN)]_2$ $2ClO_4$

Identification code	shelxl
Empirical formula	C_{24} H_{34} C_{l2} Cu_2 N_4 O_{10}
Formula weight	736.53
Temperature	293(2) K
Wavelength	0.71073 A
Crystal system, space group	Monoclinic, P21/c
Unit cell dimensions	
a	11.9790(5) A°
b	14.7940(5) A°

c	17.0060(6) A°
α	90°
β	102.0400(10)°
γ	90°
Volume	2947.46(19) A^3
Z	4
Calculated density	1.660 Mg/m^3
Absorption coefficient	1.685 mm^-1
F(000)	1512
Crystal size	0.20 x 0.20 x 0.15 mm
θ range for data collection	2.22 to 25.00 deg.
Limiting indices	$-14 \leq h \leq 14$, $-17 \leq k \leq 17$, $-20 \leq l \leq 20$
Reflections collected	26437
Unique reflections	5184 [R(int) = 0.0304]
Completeness to θ	25.00 100.0 %
Absorption correction	Semi-empirical from equivalents
Max. and min. transmission	0.7942 and 0.7190
Refinement method	Full-matrix least-squares on F^2
Data / restraints / parameters	5184 / 70 / 426
Goodness-of-fit on F^2	1.039
Final R indices [I>2 σ (I)]	$R_1 = 0.0281$, $wR_2 = 0.0694$
R indices (all data)	$R_1 = 0.0372$, $wR_2 = 0.0755$
Largest diff. peak and hole	0.621 and -0.289 $e.A^{-3}$

Table 5.6. Selected bond lengths (Å) for $[Cu(SAPEN)]_2\ 2ClO_4$

N(1)-Cu(1)	2.004(2)
N(2)-Cu(1)	1.931(2)
N(3)-Cu(2)	2.005(2)
N(4)-Cu(2)	1.923(2)
O(1)-Cu(1)	1.9299(17)
O(1)-Cu(2)	1.9420(16)
O(2)-Cu(2)	1.9435(17)
O(2)-Cu(1)	1.9655(16)
Cu(1)-Cu(2)	2.9278(4)

Table. 5.7: Selected bond angles (^{o}) for $[Cu(SAPEN)]_2\ 2ClO_4$

C(10)-N(1)-Cu(1)	117.52(16)
Cu(1)-N(1)-H(1A)	107.9(19)
C(7)-N(2)-Cu(1)	126.6(2)
C(8)-N(2)-Cu(1)	112.55(18)
C(21)-N(3)-Cu(2)	104.63(16)
C(22)-N(3)-Cu(2)	118.66(16)
Cu(2)-N(3)-H(3A)	106.6(19)
C(19)-N(4)-Cu(2)	126.62(18)
C(20)-N(4)-Cu(2)	111.97(16)
C(1)-O(1)-Cu(1)	127.55(16)
C(1)-O(1)-Cu(2)	134.09(16)
Cu(1)-O(1)-Cu(2)	98.25(7)
C(13)-O(2)-Cu(2)	128.10(15)
C(13)-O(2)-Cu(1)	134.88(16)

Cu(2)-O(2)-Cu(1)	97.00(7)
O(1)-Cu(1)-N(2)	90.88(8)
O(1)-Cu(1)-O(2)	78.04(7)
N(2)-Cu(1)-O(2)	168.91(8)
O(1)-Cu(1)-N(1)	163.58(9)
N(2)-Cu(1)-N(1)	85.82(9)
O(2)-Cu(1)-N(1)	104.87(8)
O(1)-Cu(1)-Cu(2)	41.03(5)
N(2)-Cu(1)-Cu(2)	128.42(7)
O(2)-Cu(1)-Cu(2)	41.21(5)
N(1)-Cu(1)-Cu(2)	133.79(7)
N(4)-Cu(2)-O(1)	167.01(8)
N(4)-Cu(2)-O(2)	92.33(8)
O(1)-Cu(2)-O(2)	78.28(7)
N(4)-Cu(2)-N(3)	86.31(9)
O(1)-Cu(2)-N(3)	104.20(8)
O(2)-Cu(2)-N(3)	172.15(8)
N(4)-Cu(2)-Cu(1)	132.85(7)
O(1)-Cu(2)-Cu(1)	40.72(5)
O(2)-Cu(2)-Cu(1)	41.78(5)
N(3)-Cu(2)-Cu(1)	137.30(6)

Table 5.8: Hydrogen bonds for $[Cu(SAPEN)]_2\ 2ClO_4$ [A and deg.].

D-H...A	d(D-H)	d(H...A)	d(D...A)	<(DHA)
N(1)-H(1A)...O(6')#1	0.835(17)	2.26(3)	3.082(18)	170(3)
N(1)-H(1A)...O(6)#1	0.835(17)	2.28(2)	3.084(6)	162(2)
N(3)-H(3A)...O(3)	0.825(17)	2.233(19)	3.037(6)	165(3)
N(3)-H(3A)...O(4')	0.825(17)	2.34(3)	3.03(2)	141(3)

Symmetry transformations used to generate equivalent atoms:

#1 x+1,y,z

The single crystal x-ray diffraction analysis confirms the structure suggested in **Fig 5.4** based on physico-chemical and spectral analysis.

h. Electrochemical studies:

Redox behavior of the copper(II) complexes has been investigated by cyclic voltammetry in DMF using 0.1M tetrabutylammoniumhexaflourophosphate (TBAHEP) as supporting electrolyte. The cyclic voltammetric profile of $[Cu(HAPPEN)\ (H_2O)_2]NO_3$ at different scan rates is given in **Fig 5.7**. The electrochemical data of copper(II) complexes are presented in **Table 5.9.**

Repeated scans at various scan rates suggest the presence of stable redox species in solution. $E_{1/2}$ values of all complexes observed in the potential range of 0.322 – 0.397 V vs. Ag/AgCl [9-11]. It may be inferred that all the Cu(II) complexes undergo reduction to their respective Cu(I) complexes. Though the complexes are dimers, only one wave is observed

corresponding to Cu(II) → Cu(I) reduction. This behaviour clearly suggests that the both copper centers in the molecule have same or similar coordination environment. The non-equivalent current in cathodic and anodic peaks (i_c/i_a= 0.326 and 0.812 at 100 mVs^{-1}) for complexes indicate quasi-reversible behavior [12]. The difference $\Delta E_p = E_{pc} - E_{pa}$ in all the complexes exceeds the Nerstian requirement 59/n mV (n= number of electrons involved in oxidation reduction) which suggests quasi-reversible character associated with a considerable reorganization of the coordination sphere during electron transfer [13]. The complexes have large separation (285 - 458 mv) between anodic and cathodic peaks indicating quasi-reversible character. There is an inverse relation between the $E_{1/2}$ values of copper complexes and the size of the complexes. The $E_{1/2}$ values of the complexes decrease, as the molecular weight of the complex increases [14].

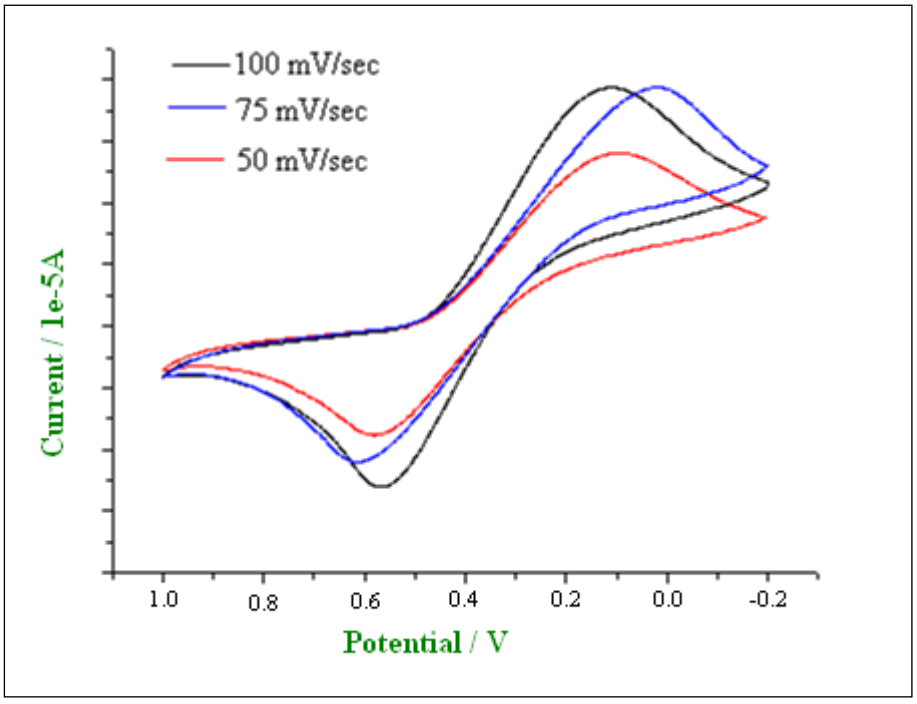

Fig 5.7: cyclic voltammetric profile of $[Cu(SAPEN)]_2$ $2ClO_4$ at different scan rates 50, 75 and 100 mVs^{-1}

Table 5.9:
Cyclic voltammetric data of copper(II) complexes

Complex	Redox couple	E_{pc} V	E_{pa} V	ΔE_p (mV)	$E_{1/2}$	$-i_c/i_a$	log K_c [a]	$-\Delta G^o$ [b]
$[Cu(SAMEN)]_2 2ClO_4$	II/I	0.168	0.626	458	0.397	0.326	0.0733	420
$[Cu(SAPEN)]_2\ 2ClO_4$	II/I	0.146	0.582	436	0.364	0.452	0.0770	442
$[Cu(HAPMEN)]_2 2ClO_4$	II/I	0.218	0.546	328	0.382	0.658	0.1024	588
$[Cu(HAPPEN)]_2\ 2ClO_4$	II/I	0.107	0.537	285	0.322	0.812	0.1178	676

[a] $\log K_c = 0.434\ ZF/RT\Delta E_p$; [b] $\Delta G^o = -2.303\ RT \log K_c$

i. DNA binding studies of copper(II) complexes

The interaction of metal complexes with calf-thymus DNA was monitored by UV-visible spectroscopy. The absorption spectra of complexes were compared in the absence and in the presence of CT-DNA. In the presence of increasing amounts of DNA, the spectra of all complexes showed a strong decrease (Hypochromicity) or increase (Hyperchromicity) in intensity with shift in absorption maxima towards lower (blue-shift) or higher (red-shift) wavelengths. The change in absorbance values with increasing amount of CT-DNA were used to evaluate the intrinsic binding constant K_b for the complex.

Copper(II) complexes exhibit an intense absorption band around 341-368 nm which is attributed to metal-ligand charge transfer (MLCT) transitions. Absorption spectra were recorded in the range of 250-500 nm. Electronic absorption spectral data upon addition of

CT-DNA and binding constants of these complexes are given in the Table 5.10. The change in absorbance values with increasing amounts of CT-DNA was used to evaluate the intrinsic binding constant K_b, for the complexes. In the presence of increasing amounts of CT-DNA, the UV-Visible absorption spectra of copper (II) complexes show bathochromic shift (λ_{max}: 1-7 nm). It is evident from the table, that all the complexes bind with DNA with high affinities and, the estimated binding constants are in the range 1.15 to 2.24 x 10^5 M^{-1}. This may be due to the presence of pi- stacking of the phenyl ring present in the Schiff base ligand. Typical absorption spectra of $[Cu(HAPMEN)]_2 2ClO_4$ in presence and in absence of DNA are shown in **Fig 5.8**. The binding constants (K_b) for DNA interaction of the complexes have been calculated by using the following equation:

$$[DNA] / (\varepsilon_a - \varepsilon_f) = [DNA] / (\varepsilon_b - \varepsilon_f) + 1/ K_b (\varepsilon_b - \varepsilon_f) \qquad (1)$$

From **Table 5.10** the order of binding constants of present copper complexes may be given as:

$[Cu(HAPPEN)]_2 2ClO_4 < [Cu(SAPEN)]_2 2ClO_4 < [Cu(HAPMEN)]_2 2ClO_4 < [Cu(SAMEN)]_2 2ClO_4$

1.15 x 10^5 1.25 x 10^5 1.68 x 10^5 2.24 x 10^5

$[Cu(HAPPEN)]_2$ $2ClO_4$ exhibits the least binding constant and $[Cu(SAMEN)]_2 2ClO_4$ shows highest binding constant. This gives a clear idea that complexes with higher molecular weight show lesser binding constants. This may be due to presence of bulky ligand moieties which cause steric hindrance. The binding constants of the present dinuclear complexes are less than those of mononuclear copper(II) complexes (derived from the same ligands which are discussed in Chapter-4). This may be due to the bulky nature of dinuclear complexes. Mononuclear complexes contain coordinated water molecules which are regardes as labile ligands. On the addition of DNA, mononuclear complexes undergo substitution reaction replacing coordinated water molecules with DNA bases.

Table 5.10:

Electronic absorption data upon addition of CT-DNA to Cu (II) complexes

Complex	$\lambda_{max/nm}$		Δλ/nm	H%	$K_b(M^{-1})$	$K_b(M^{-1})$*
	Free	Bound				
$[Cu(SAMEN)]_2\ 2ClO_4$	368	361	7	11.23	2.24×10^5	9.91×10^6
$[Cu(SAPEN)]_2\ 2ClO_4$	352	349	3	18.21	1.25×10^5	9.25×10^6
$[Cu(HAPMEN)]_2 2ClO_4$	346	344	2	12.25	1.68×10^5	8.68×10^6
$[Cu(HAPPEN)]_2\ 2ClO_4$	341	342	1	16.36	1.15×10^5	8.36×10^6

*Binding constants of corresponding mononuclear complexes

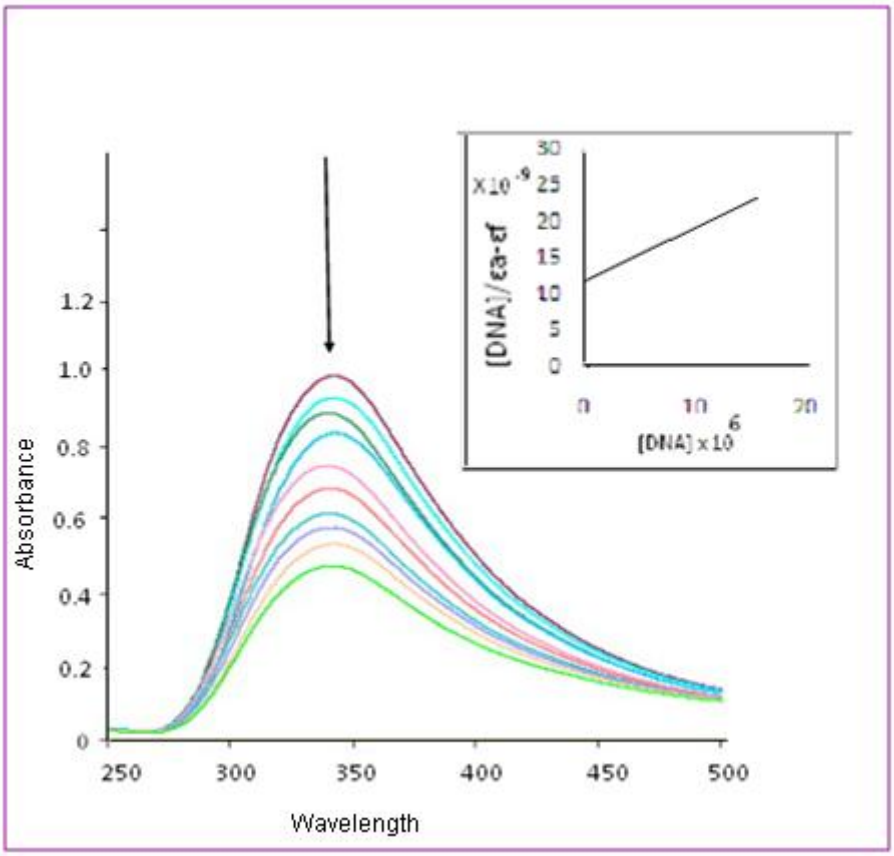

Fig 5.8: **Absorption spectra of $[Cu(HAPMEN)]_2 2ClO_4$ in the absence and in the presence of increasing concentration of CT-DNA; top most spectrum is recorded in the absence of DNA; A plot of $[DNA]/(\varepsilon_a-\varepsilon_f)$ versus [DNA] is shown in the inset**

j. DNA cleavage activities of copper(II) complexes

Nuclease activity of dinuclear copper(II) complexes derived from tridentate Schiff base ligands has been studied by agarose gel electrophoresis using pBR 322 plasmid DNA in Tris-HCl/NaCl (50mM / 5mM) buffer (pH-7) in the presence and absence of H_2O_2 after 30 minutes incubation period at 37°C [15,16]. Nuclease activity of complexes was also investigated in presence of free radical scavenger (DMSO), chelating agent (EDTA) and reducing agent DTT. In the absence of H_2O_2 the complexes cleaved supercoiled DNA (Form 1) into nicked DNA (Form II) (**Fig. 5.9** and **5.10**, lane 3 and 8). From **Fig 5.9** (lanes 4 & 9) and **Fig 5.10** (lanes 4 & 9) it is evident that copper complexes cleave DNA more effectively in the presence of oxidant which may be due to hydroxyl radical (OH) reaction with DNA. This is consistent with the increased production of hydroxyl radicals by cuprous ions similar to the well known Fenton reaction [17]. Nuclease activity of copper (II) complexes decreases with their molecular weights. This may be due to the presence of bulky ligand moities present in the complexes. Higher nuclease activity of copper(II) complexes of lower molecular weights may also be attributed due to their favourable redox potential values. Complexes with higher $E_{1/2}$ values exhibit higher nuclease activity.

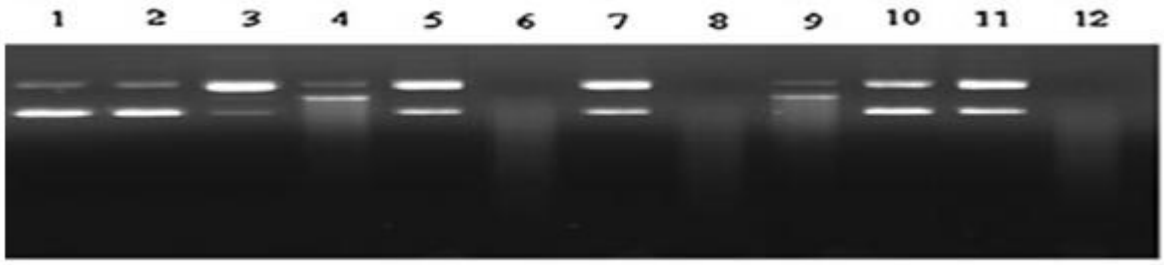

Fig 5.9: Agarose gel (0.8%) showing results of electrophoresis of 1µl of pBR 322 Plasmid DNA; 4µl of Tris-HCl/NaCl (50mM/5mM) buffer (pH-7); 2µl of complex in DMF($1x10^{-3}$M); 11µl of sterilized water; 2µl of H_2O_2 (total volume 20µl) were added, respectively, incubated at 37^0C (30 min);
Lane 1: DNA control; Lane 2: DNA control + H_2O_2; Lane 3: $[Cu(SAMEN)]_2 2ClO_4$+ DNA; Lane 4: $[Cu(SAMEN)]_2 2ClO_4$+ DNA+ H_2O_2; Lane 5: $[Cu(SAMEN)]_2 2ClO_4$+ DNA+DMSO; Lane 6: $[Cu(SAMEN)]_2 2ClO_4$+ DNA + EDTA; Lane 7: $[Cu(SAMEN)]_2 2ClO_4$+ DNA+DTT; Lane 8: $[Cu(SAPEN)]_2$ $2ClO_4$+ DNA; Lane 9: $[Cu(SAPEN)]_2$ $2ClO_4$+ DNA+ H_2O_2; Lane 10: $[Cu(SAPEN)]_2$ $2ClO_4$+ DNA+DMSO; Lane 11: $[Cu(SAPEN)]_2$ $2ClO_4$+ DNA+ EDTA; Lane 12: $[Cu(SAPEN)]_2$ $2ClO_4$+ DNA+DTT;

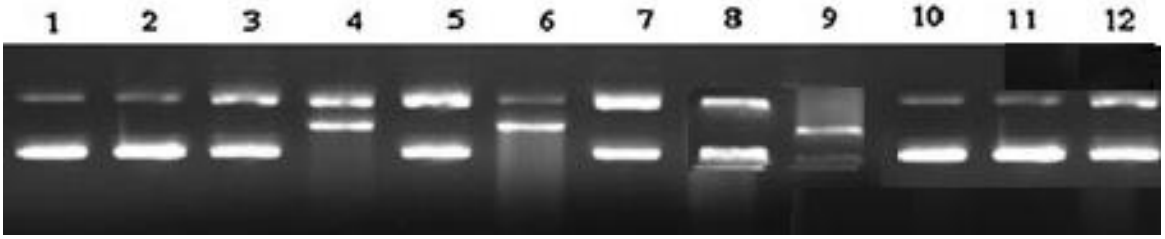

Fig 5.10: Agarose gel (0.8%) showing results of electrophoresis of 1µl of pBR 322 Plasmid DNA; 4µl of Tris-HCl/NaCl (50mM/5mM) buffer (pH-7); 2µl of complex in DMF($1x10^{-3}$M); 11µl of sterilized water; 2µl of H_2O_2 (total volume 20µl) were added, respectively, incubated at 37^0C (30 min);
Lane 1: DNA control; Lane 2: DNA control + H_2O_2; Lane 3: $[Cu(HAPMEN)]_2 2ClO_4$+ DNA; Lane 4: $[Cu(HAPMEN)]_2 2ClO_4$+ DNA+ H_2O_2; Lane 5: $[Cu(HAPMEN)]_2 2ClO_4$+ DNA+DMSO; Lane 6: $[Cu(HAPMEN)]_2 2ClO_4$ + DNA + EDTA; Lane 7: $[Cu(HAPMEN)]_2 2ClO_4$ + DNA+DTT; Lane 8: $[Cu(HAPPEN)]_2 2ClO_4$+ DNA; Lane 9: $[Cu(HAPPEN)]_2 2ClO_4$+ DNA+ H_2O_2; Lane 10: $[Cu(HAPPEN)]_2 2ClO_4$+ DNA+DMSO; Lane 11: $[Cu(HAPPEN)]_2 2ClO_4$+ DNA+ EDTA; Lane 12: $[Cu(HAPPEN)]_2 2ClO_4$+ DNA+DTT;

k. Cytotoxic activity of copper(II) complexes

The MTT assay was done to check for the cytotoxic activity of the compounds on MCF-7 (a human breast carcinoma).

As all the present copper(II) complexes exhibit considerable DNA binding and cleavage activity, as most of the redox-active metal complexes showing DNA cleavage activity exhibit anticancer activity the cytotoxicity of the complexes against the MCF-7 human breast cancer cell line was investigated by using MTT assay. The MTT Cell Proliferation and Viability Assay is a safe, sensitive, *in vitro* assay for the measurement of cell proliferation or, when metabolic events lead to apoptosis or necrosis, a reduction in cell viability. 5000 cells are plated in quadruplets at 100 μL/well for each variable in a 96-well tissue culture plates. Then the cells are treated with various concentrations of copper complexes after incubating at 37 °C for 16-18 h. 20 μL of MTT reagent (2.5 mg/ml) and 80 μl of medium are added to each well and further incubated for 2-4 hours at 37 °C. When purple precipitate is clearly visible under the microscope, 100 μL of isopropanol is added to all wells, including control wells. The absorbance of the wells is measured at 570 nm, including the blank (100 μl isopropanol). A graph of absorbance versus treatment was plotted. The IC_{50} value defined as the drug concentration that resulted in a 50% reduction in cell numbers compared to untreated controls was measured by plotting the percentage cytotoxicity versus concentration on a logarithmic graph by means of Eq. (1):

$$\% \text{ cell inhibition} = 100 - \text{Abs(sample)}/\text{Abs(control)} \times 100 \quad (1)$$

The IC_{50} values obtained by plotting the cell viability against concentration of the complexes reveal that all of them exhibit least cytotoxicity after 24 h incubation. **Fig 5.11** show the cytotoxic effect (% cell inhibition) of $[Cu(SAPEN)]_2 2ClO_4$. **Fig 5.12** displays the

variation in the IC_{50} values of mono and dinuclear complexes. **Table 5.11** gives the details of percentage of ratio of absorbance in sample well and absorbance in control well [Abs(sample)/Abs(control) × 100] and percentage of cell inhibition or viability. The calculated IC_{50} values are presented in **Table 5.12**. The values are in the range of 184.48 to 210.44 μM. Among all the complexes $[Cu(SAMEN)]_2 2ClO_4$ shows the highest cytotoxicity. The data suggest that the cytotoxicity of the complexes is inversely proportional to their molecular weights. However the data reveal that cytotoxicity of the copper(II) complexes is not in good agreement with DNA binding and cleavage activity. This activity of the complexes thus suggests that *in vivo* mechanism of action of the complexes is more complicated than the one occurring for the *in vitro* DNA cleavage. The experiments indicate that cytotoxic effect of the present complexes was considerably less pronounced, since their IC_{50} values are sufficiently high.

Cytotoxic activity of the complexes does not corroborate with the in vitro binding affinity and nuclease activity of metal complexes. This indicates that, the cytotoxic activity of the complexes follow a different mechanism. The experiments reveal that further studies are needed to understand the relation of nuclease activity and cytotoxic effect of these complexes.

Table 5.11:

In vitro cytotoxicity of the Cu(II) complexes in human breast (MCF7) cancer cell lines – Cell inhibition percentage

Concentration	$[Cu(SAPEN)]_2 2ClO_4$		$[Cu(SAPEN)]_2 2ClO_4$		$[Cu(HAPMEN)]_2 2ClO_4$		$[Cu(HAPPEN)]_2 2ClO_4$	
	%OD	%IC	%OD	%IC	%OD	%IC	%OD	%IC
25 μg/ml	96.17	03.83	96.73	03.26	91.77	08.22	--	--
50 μg/ml	88.35	11.64	92.78	07.21	91.32	08.67	--	--
100 μg/ml	88.06	11.91	88.17	11.83	81.63	18.36	--	--

Table 5.12:

In vitro cytotoxicity of the Cu(II) complexes in human breast (MCF7) cancer cell lines – IC_{50} values of copper complexes

Complex	**IC_{50} value (μM)**
$[Cu(SAMEN)]_2 2ClO_4$(**1**)	184.48
$[Cu(SAPEN)]_2 2ClO_4$ (**2**)	210.44
$[Cu(HAPMEN)]_2 2ClO_4$ (**3**)	192.23
$[Cu(HAPPEN)]_2 2ClO_4$(**4**)	ND

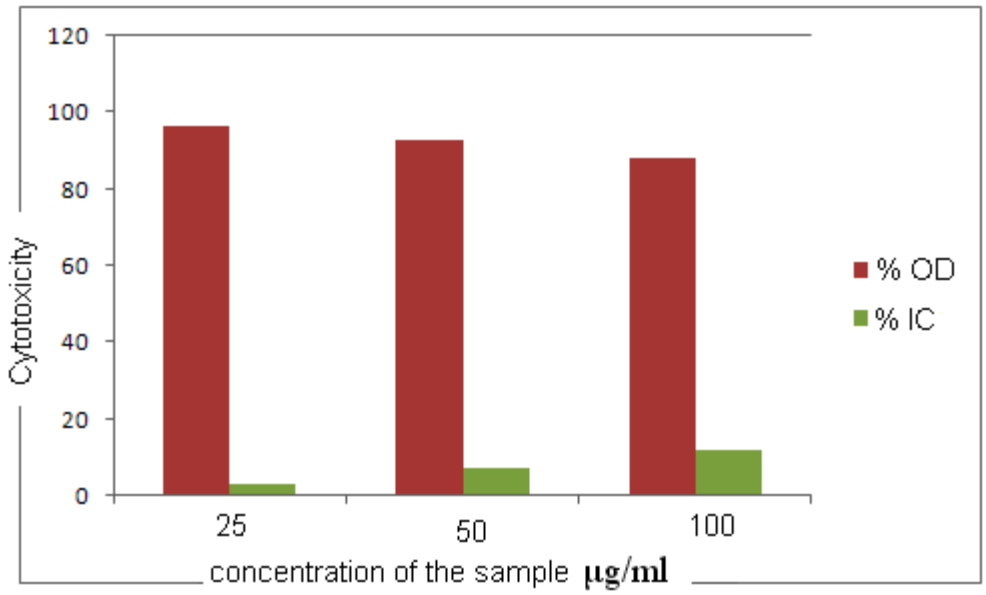

Fig 5.11: *In vitro* cytotoxicity of $[Cu(SAPEN)]_2\ 2ClO_4$ in human breast (MCF7) cancer cell lines – percentage of cell inhibition

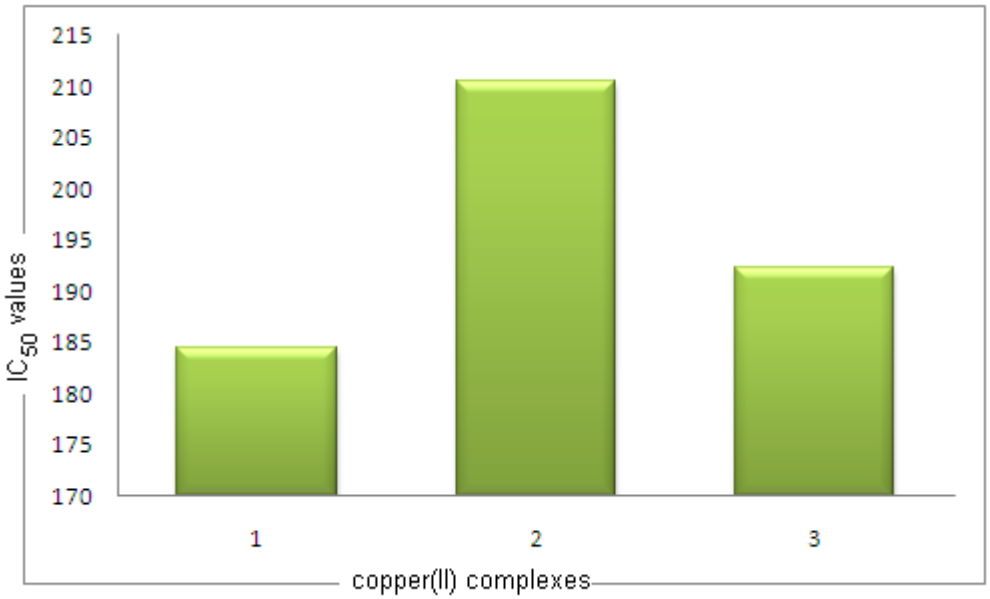

Fig 5.12: *In vitro* cytotoxicity of the Cu(II) complexes in human breast (MCF7) cancer cell lines - IC_{50} values of copper complexes

References:

1. K.Hussain Reddy, M.Surendra Babu, P.Suresh Babu, S.Dayananda, *Indian J Chem. Technol.,* 11 (**2004**) 29.
2. S. Anbu, M. Kandaswamy, *Polyhedron* 30 (**2011**) 123.
3. A.B.P. Lever, *"Inorganic Electronic Spectroscopy",* 2nd Edn. (Elsevier, Amsterdam) (**1984**).
4. K. Hussain Reddy, Y. Lingappa, *Trans. Met. Chem*., 19 (**1994**) 487.
5. B. Sarkar, M.S. Ray, M.G.B. Drew, A. Figuerola, C. Diaz, A. Ghosh, *Polyhedron,* 25 (**2006**) 3084
6. B. Sarkar, M.S. Ray, Y.-Z Li, Y. Song, A. Figuerola, E. Ruiz, J. Cirera, J. Cano, A. Ghosh, *Chem. Eur. J.* 13 (**2007**) 9297.
7. B.J.Hathaway and D.E. Billing, *Coord. Chem. Rev.,* 5 **(1961)** 143.
8. D. Kivelson, R. Neiman, *J. Chem. Phys.,*35, **(1961)** 149–155.
9. X.H. Bu, Z.H. Zhang, X. Cao, S. Ma and Y. Tichen. *Polyhedron* 16 **(1997),** p. *3525*.
10. S Dhar, D Senapathi, P.K. Das, P Chattopadyay, M Nethaji, AR Chakravarthy, *J. Am.Chem. Soc* 125 **(2003)** 12218.
11. S.Djebbar-Sid, O.Benali-Baitich and J P Deloume, *Polyhedron,* 16, **(1997)** 2175.
12. A.A.Khumhar, S.B.Rendye, D.X. West, A.E.Libert, *Tran. Met. Chem.*. 16, **(1991),** 276.
13. S.Usha, M.Palaniandavar, *J. chem. Soc., Dalton Trans*., (**1994**), 2277.
14. P.Muralikrishna, *Ph.D., thesis*, S.K.University, Anantapur, **2007.**
15. P.Murali Krishna, K.Hussain Reddy, J P Pandey, S.Dayananda, *Trans. Met. Chem.* **(2008)** 33:661
16. P. Haribabu, Y. P. Patil, K Hussain Reddy, M. Nethaji, *Trans. Met. Chem.*36, 8 **(2011),** 867-874.
17. A.Hangan, A.Bodiki, L.Oprean, G.Alzuet, M.L. Gpnzalez, J.Borras., *Polyhedron,* 29, (**2010)** 1305.